

Research Article

Effect of Rheological Mesoparameters on Shear Mechanical Behavior of Joints

Kefeng Zhou ¹, Sheng Liu,¹ and Yanhui Cheng^{2,3}

¹School of Traffic and Transportation Engineering, Changsha University of Science and Technology, Changsha Hunan 410114, China

²School of Civil Engineering, Hunan City University, Yiyang, Hunan 413000, China

³School of Resource Safety Engineering, Central South University, Changsha, Hunan 410083, China

Correspondence should be addressed to Kefeng Zhou; zkf1978@126.com

Received 2 January 2022; Accepted 14 March 2022; Published 30 March 2022

Academic Editor: Zhijie Wen

Copyright © 2022 Kefeng Zhou et al. This is an open access article distributed under the Creative Commons Attribution License, which permits unrestricted use, distribution, and reproduction in any medium, provided the original work is properly cited.

Under natural conditions, joint failure usually occurs after long-term loading rather than short-term loading. In order to prevent rock mass failure caused by creep behavior, bolt is widely used as a mature and effective reinforcement method. Therefore, it is necessary to consider the rheological effect of bolted joint. In this paper, the particle flow code (PFC) was used to study the effect of mesoparameters on the rheological shear mechanical behavior of joints without bolts and with bolts. The effects of mesoparameters such as Maxwell elastic coefficient E_m , Maxwell viscosity coefficient C_m , Kelvin elastic coefficient E_k , Kelvin viscosity coefficient C_k , and friction coefficient F_s were analyzed. The results show that E_m and F_s mainly affect the instantaneous shear displacement, but have little effect on the rheological shear displacement. However, C_m , E_k , and C_k have little effect on the instantaneous shear displacement, and the sensitivity is mainly reflected in the rheological shear displacement. E_m and F_s mainly affect the instantaneous shear displacement, but have little effect on the rheological shear displacement. However, C_m , E_k , and C_k have little effect on the instantaneous shear displacement, and the sensitivity is mainly reflected in the rheological shear displacement. Compared with the parameter sensitivity characteristics without bolt, the instantaneous shear displacement, shear stiffness, and steady rheological displacement under anchor condition are less affected by parameters, indicating that anchor can reduce the influence of joint parameters.

1. Introduction

The mechanical properties of joints are important factors affecting the stability of rock mass engineering [1–3]. Under natural conditions, joint failure usually occurs after long-term loading rather than short-term loading. Under the condition of constant external stress, the displacement and stress field of joint are constantly adjusted and reorganized with time, resulting in the creep phenomenon that the strain increases continuously with time, which leads to the failure of jointed rock mass [4–6]. In order to prevent rock mass failure caused by creep behavior, bolt is widely used as a mature and effective reinforcement method [7, 8]. The mechanical properties of bolted joints can be studied by experiment, theoretical analysis, and numerical simulation [9–13]. At present, numerical calculation methods have been

widely used in the field of rock mechanics, forming a variety of numerical calculation methods, including finite element method, discrete element method, motion element method, and meshless method [14–16]. Each method has its own advantages and disadvantages, which can solve geotechnical engineering-related problems. In the process of joint shear, due to the fluctuation of rock rupture, the cracks will occur in the rock mass and lead to stress and strain change [17–19]. However, the numerical calculation method based on continuum cannot easily simulate crack development, joint shear slip of continuous deformation of the line. Therefore, it is necessary to consider the material discontinuity numerical calculation method, such as particle flow code (PFC) [20, 21]. In order to study the mesomechanical characteristics of bolted joints, some scholars adopted PFC to simulate the macroscopic mechanical response of bolted

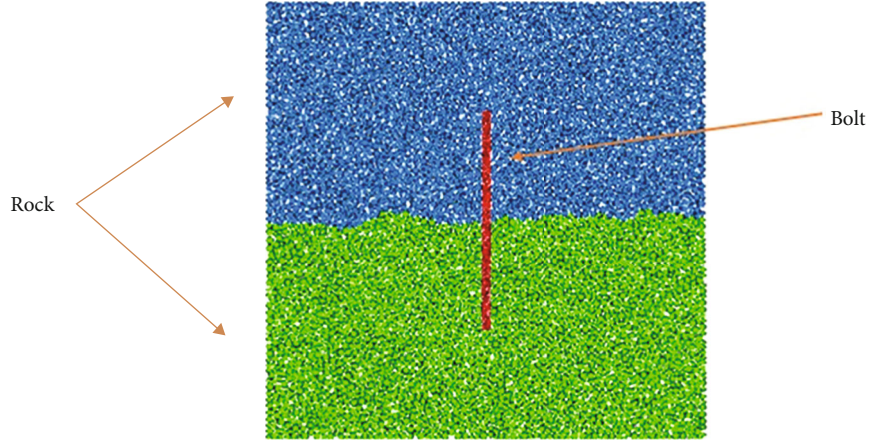


FIGURE 1: Numerical model of bolted joint subjected to rheological direct shear.

TABLE 1: Mesoscopic parameters of the numerical model.

Category	Microparameter (unit)	Value
Particle	Density (kg/m^3)	2500
	Radius (mm)	0.48-0.9
	f	5.0
	Krat (kn/ks)	0.5
	Porosity	0.16
Flat-joint contact model	Emod (10^9)	0.425
	fj_ten (10^6)	4.10
	fj_coh (10^6)	20.8
	fj_fa ($^\circ$)	58.47
	fj_n	4
Burger contact model	bur_knm (10^9)	0.06
	bur_ksm (10^9)	0.06
	bur_cnm (10^9)	12.4
	bur_csm (10^9)	12.4
	bur_knk (10^9)	1.6
	bur_ksk (10^9)	1.6
	bur_cnk (10^9)	13.1
	bur_csk (10^9)	13.1
bur_fs	0.6	

joints through the interaction between mesoparticles. Shang et al. [22] established a numerical calculation model of discontinuous joints, studied the characteristics of joint mesoscopic parameters, and simulated the failure mode and strength characteristics of joints under equal normal stress and equal normal stiffness. The previous work mainly studied the shear mechanical properties of joints under conventional conditions, and the rheological effects of joint shear were seldom considered. Therefore, this paper adopts discrete element numerical calculation method to conduct rheological shear simulation tests on both anchored and unbolted joints and adopts control variable method in parameter sensitivity analysis. The effects of rheological mesoscopic parameters such as Maxwell body elastic coefficient

E_m , Maxwell body viscosity coefficient C_m , Kelvin body elastic coefficient E_m , Kelvin body viscosity coefficient C_m , and friction coefficient F_s on shear mechanical behavior of joints were investigated.

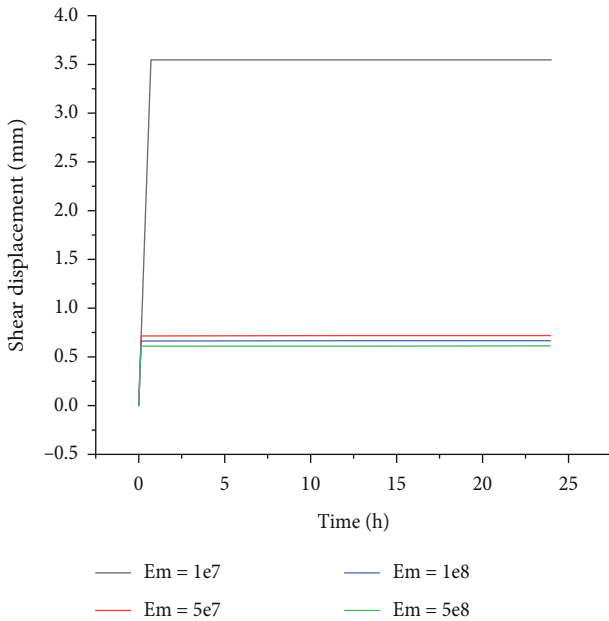
2. Numerical Model

The numerical calculation model of joint was established using PFC, and the size of the model was $100 \text{ mm} \times 100 \text{ mm}$. Based on the established intact rock mass geometry model, the corresponding joint geometry is drawn in CAD. The geometry is imported into PFC by the geometry import command, and it is set to DFN fracture to establish the rock mass geometry model with joints. In the model, different particle parameters are set to simulate the bolt, as shown in Figure 1. In this paper, a flat-joint model is used to simulate the upper and lower rock blocks. Due to shear box in the rheological shear test parts in addition to a constant load, loading wall outside wall is consistent with the only wall loading rate of unconstrained free wall.

In the study of shear mechanical behavior, the experimental phenomenon at the moment of peak shear displacement is an important research object, and it is necessary to keep the simulated peak shear displacement consistent with the real test as much as possible [23–25]. Therefore, in this paper, the results of numerical simulation when normal stress is 1 MPa and laboratory test are the same as the standard, and the trial-and-error method is adopted to calibrate the mesoscopic parameters of rock. Firstly, a complete sample numerical model of flat joints is established to simulate the shear stress-shear displacement curve of flat joints. Finally, the mesoscopic parameters matching the actual situation are calibrated. The microscopic parameters of the numerical model are shown in Table 1. According to the bolt parameters in reference [26], a parallel bond model is used to describe the bolt. The friction coefficient is 0.5, which is smaller than that of rock. The tensile strength of bolt particles is 4.0 GPa, the bond force is 0.9 GPa, and the internal friction angle is 20° . Set a 5 cm long bolt with a diameter of 2 mm, as shown in Table 2 for specific parameters.

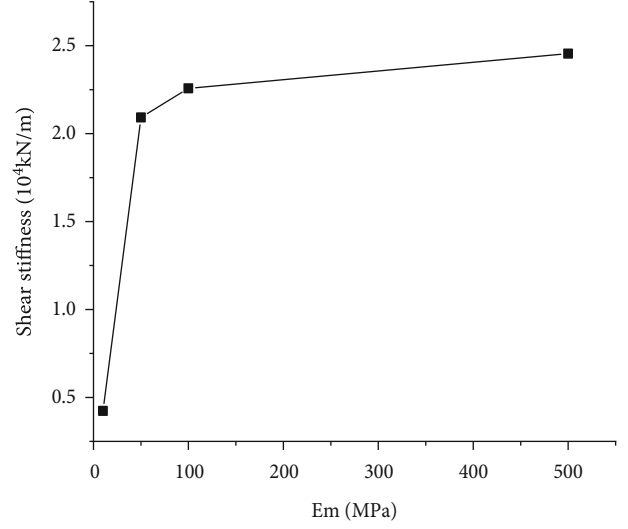
TABLE 2: Mesoscopic parameters of bolt.

Category	Mesoscopic parameters	Value
Particle	Density (kg/m^3)	7850
	Radius (mm)	0.18-0.3
	f	0.5
	Porosity P	0.16
	Normal stiffness k_n	$8e9$
	Shear stiffness k_s	$2.286e9$
Flat-joint contact model	Tensile strength pb_ten (GPa)	4.25
	Cohesion pb_coh (MPa)	900
	Friction angle pb_fa ($^\circ$)	0
	Normal stiffness pb_k_n	$5.9e14$
	Shear stiffness pb_k_s	$5.9e14$

FIGURE 2: Shear displacement-time relation of unbolted joints under different E_m .

3. Calculation Results and Analysis

3.1. Relationship between Maxwell Elastic Coefficient and Macroscopic Shear Stiffness. In the rheological contact model, Maxwell volume elastic coefficient E_m controls the instantaneous displacement of intergranular contact. It is of important reference value to analyze the influence of E_m , the microscopic parameter of intergranular contact, on the macroscopic shear mechanical properties of joints. The control variable method was adopted, set to $1E7$, $5E7$, $1E8$, and $5E8$ (unit: Pa), respectively, to analyze the sensitivity of elastic coefficient E_m of Maxwell body. Shear displacement-time curves of bolt-free joints under different E_m conditions are shown in Figure 2. As can be seen from the figure, the instantaneous shear displacement decreases

FIGURE 3: Relationship between E_m and macroscopic shear stiffness of joints without bolt.

with the increase of E_m , and E_m has a significant effect on the instantaneous shear displacement. Different E_m corresponds to the same rheological shear displacement, and E_m has no effect on the rheological shear displacement. By analyzing the elastic moduli corresponding to different E_m , the macroscopic shear stiffness K_s corresponding to different E_m is obtained, and the relationship between E_m and shear stiffness is shown in Figure 3. The shear stiffness is obtained from the curve of relation between shear stress and shear displacement; the curve slope represents the shear stiffness. It can be seen that there is a nonlinear relationship between E_m and macroscopic shear stiffness, and the shear stiffness changes greatly and converges to a value, indicating that E_m has a significant influence on macroscopic shear stiffness. The nonlinear expression is used to fit it, and the results are shown in Equation (1); R^2 is 0.98, indicating that the formula can well predict the macroscopic shear stiffness under different E_m conditions.

$$K_s = 3.1[1 - \exp(-0.04E_m)] - 0.719. \quad (1)$$

In the case of bolted joint, shear displacement-time curves under different E_m conditions were recorded, as shown in Figure 4. It can be seen that, similar to the case without bolt, the instantaneous shear displacement decreases with the increase of E_m , and E_m has a significant effect on the instantaneous shear displacement. Different E_m corresponds to the same rheological shear displacement, and E_m has no effect on the rheological shear displacement.

By analyzing the elastic moduli corresponding to different E_m , the macroscopic shear stiffness corresponding to different E_m is obtained, and the relationship between E_m and shear stiffness is shown in Figure 5. It can be seen that there is a nonlinear relationship between E_m and macroscopic shear stiffness, and the shear stiffness changes greatly and converges to a value, indicating that E_m has a significant influence on macroscopic shear stiffness. Nonlinear expression was used to fit them, and the results are shown in

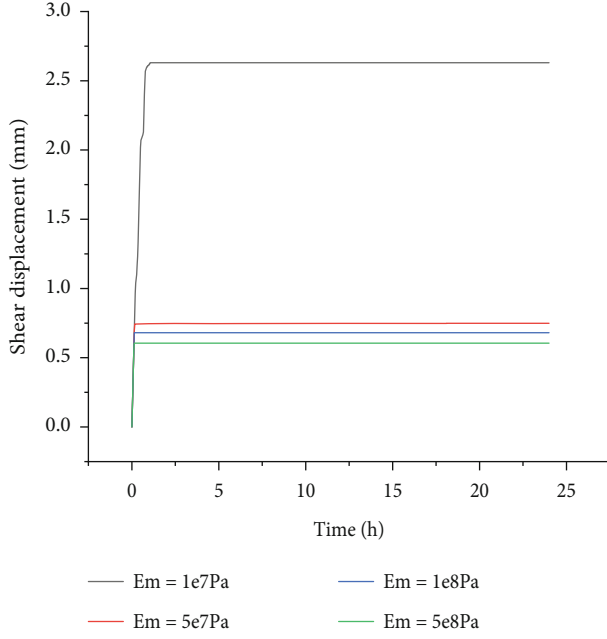


FIGURE 4: Shear displacement-time relation under different E_m with bolts.

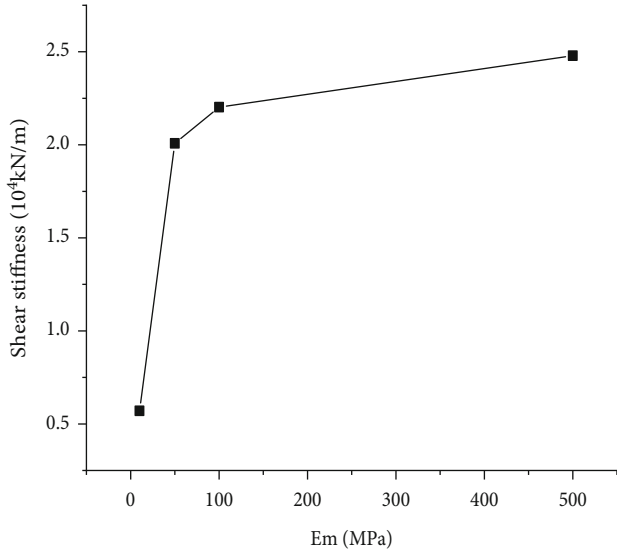


FIGURE 5: Shear stiffness of different E_m with bolt.

Equation (2). R^2 is 0.96, indicating that this formula can well predict the macroscopic shear stiffness under different E_m . Compared with Formula (1) without bolt, the shear stiffness with bolt is less affected by E_m , and the convergence value is also smaller, indicating that the bolt can reduce the influence brought by the change of joint parameters.

$$K_s = 2.6[1 - \exp(-0.03E_m)] - 0.207. \quad (2)$$

3.2. Influence of Maxwell Volume Viscosity Coefficient on the Relationship between Joint Shear Displacement and Time. In Burger's contact model, Maxwell viscosity coefficient C_m controls the creep displacement of interparticle contact,

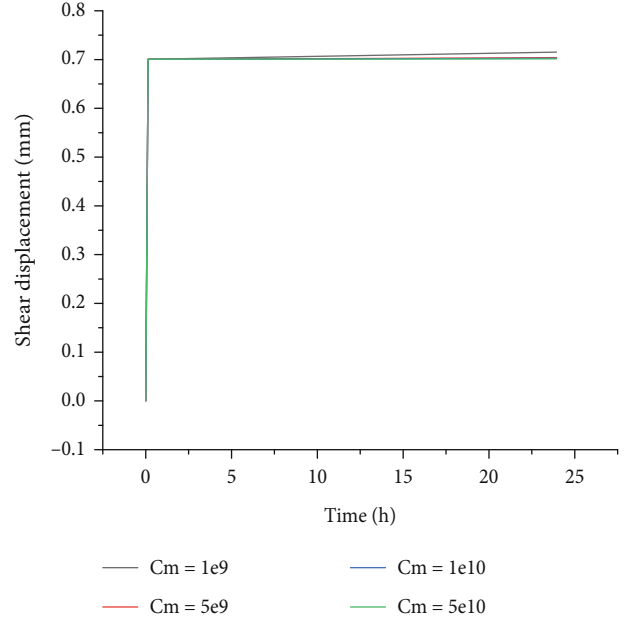


FIGURE 6: Shear displacement-time relation of unbolted joints under different C_m conditions.

and the displacement is closely related to time. Analyzing the microscopic parameter C_m of interparticle contact can effectively reflect the macroscopic mechanical characteristics of Burger's model parameters in the process of joint shear. The control variable method was adopted, set to $1E9$, $5E9$, $1E10$, and $5E10$, respectively, to analyze the sensitivity of Maxwell body viscosity coefficient C_m . The shear displacement-time curves of bolt-free joints under different C_m are shown in Figure 6. It can be seen that C_m has little influence on instantaneous shear displacement, but significant influence on rheological shear displacement. The larger C_m is, the smaller the rheological shear displacement is, and there is a negative correlation between the two. The rheological shear simulation results of unbolted joints obtained by changing C_m show that the adjustment of C_m has no significant effect on the joint numerical model displacement, crack. The results show that C_m affects the shear mechanical properties under rheological conditions, but the effect is small when no damage occurs. C_m is a factor affecting particle contact, but different from the displacement affected by E_m . The displacement affected by C_m is controlled by time. Therefore, when the time scale is not very large and C_m is not very small, the displacement affected by C_m is not particularly obvious.

In the case of bolted joint, shear displacement-time curves under different C_m conditions were recorded, as shown in Figure 7. It can be seen that C_m has little influence on instantaneous shear displacement, but significant influence on rheological shear displacement. The larger C_m is, the smaller the rheological shear displacement is, and there is a negative correlation between the two. Compared with Figure 6 without bolt, the discretization of shear displacements and time curves of different C_m in Figure 7 with bolt is smaller, indicating that anchor can reduce the influence of

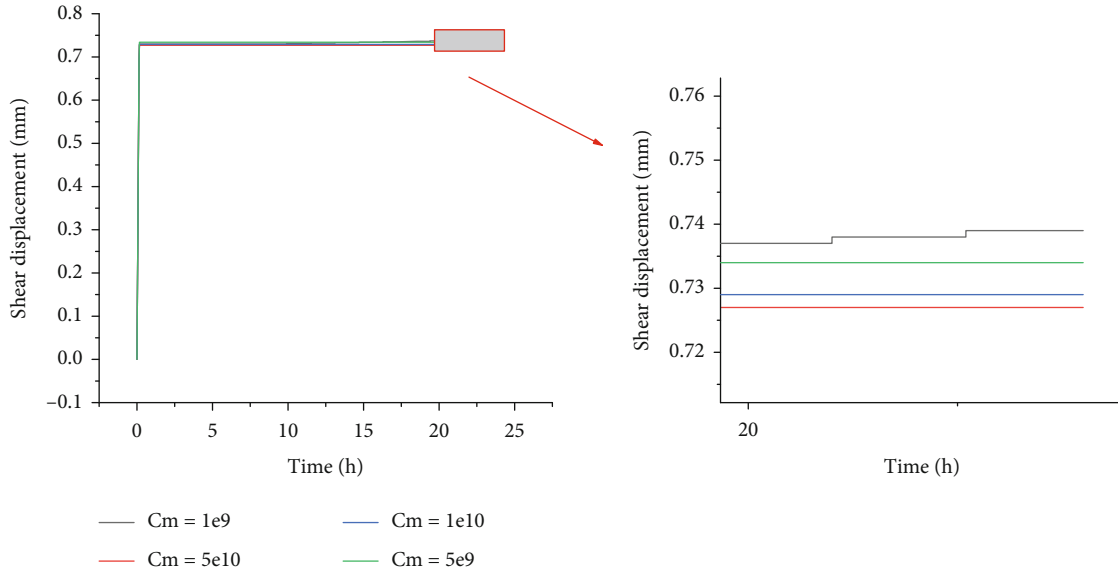


FIGURE 7: Shear displacement-time curves of bolted joints at different C_m .

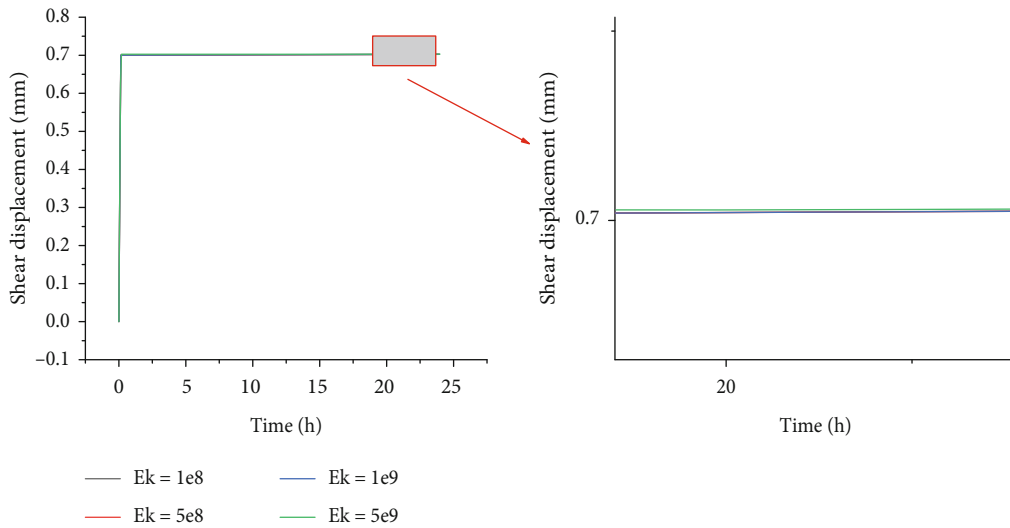


FIGURE 8: Shear displacement-time curves under different E_k conditions without bolt.

joint parameter C_m on joint aging deformation. The rheological shear simulation results of bolted joints obtained by changing C_m show that adjusting C_m has no significant effect on the joint numerical model displacement and crack. The results show that C_m affects the shear mechanical properties under rheological conditions, but the effect is small when no damage occurs. Compared with the condition without bolt, the influence of C_m on displacement is less obvious in the condition with bolt, and the influence of C_m on displacement can be weakened by bolt.

3.3. Influence of Nonlinear Kelvin Elastic Coefficient on Shear Mechanical Behavior of Joints. In the rheological contact model, the Kelvin elastic coefficient (E_k) affects the aging displacement of interparticle contact. The analysis of the micro parameter (E_k) of interparticle contact can effectively study the reflection of Burger's model parameters in macroscopic

shear mechanical properties of joints. The control variable method was adopted, set to 1E8, 5E8, 1E9, and 5E9 (unit: Pa), respectively, to analyze the sensitivity characteristics of the elastic coefficient of Kelvin body E_k . The shear displacement-time curves of boltless joints under different E_k conditions are shown in Figure 8. It can be seen that E_k has little effect on the instantaneous shear displacement, but has an obvious effect on the rheological shear displacement. The larger E_k is, the smaller the rheological shear displacement is, and there is a negative correlation between them.

The rheological shear simulation results of unbolted joints obtained by changing E_k show that adjusting E_k has no obvious effect on the numerical model displacement, crack of the joints. The results show that E_k affects the shear mechanical properties under rheological conditions, but the effect is small when no damage occurs. E_k affects particle displacement, but the displacement is controlled by time.

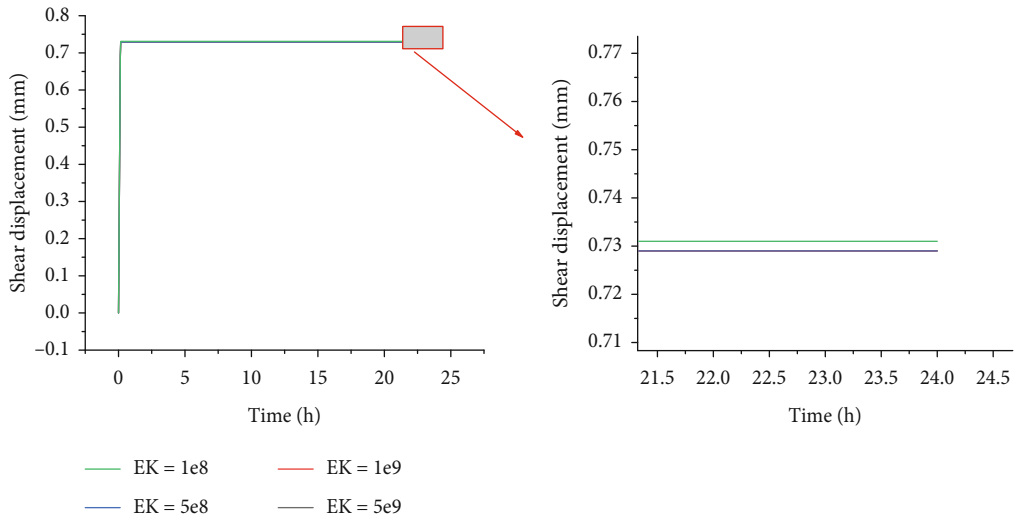


FIGURE 9: Shear displacement-time relation under different E_k conditions with bolt.

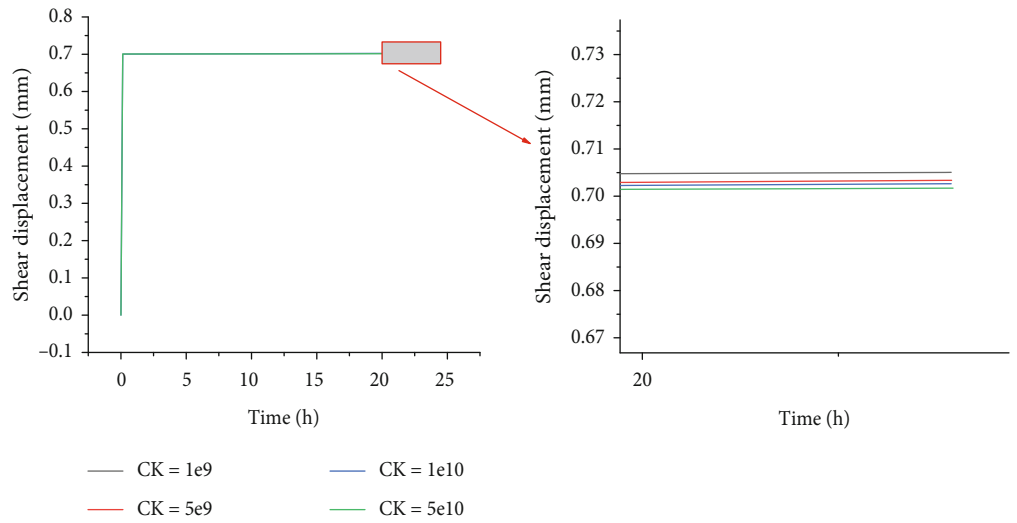


FIGURE 10: Shear displacement-time relation under different C_k .

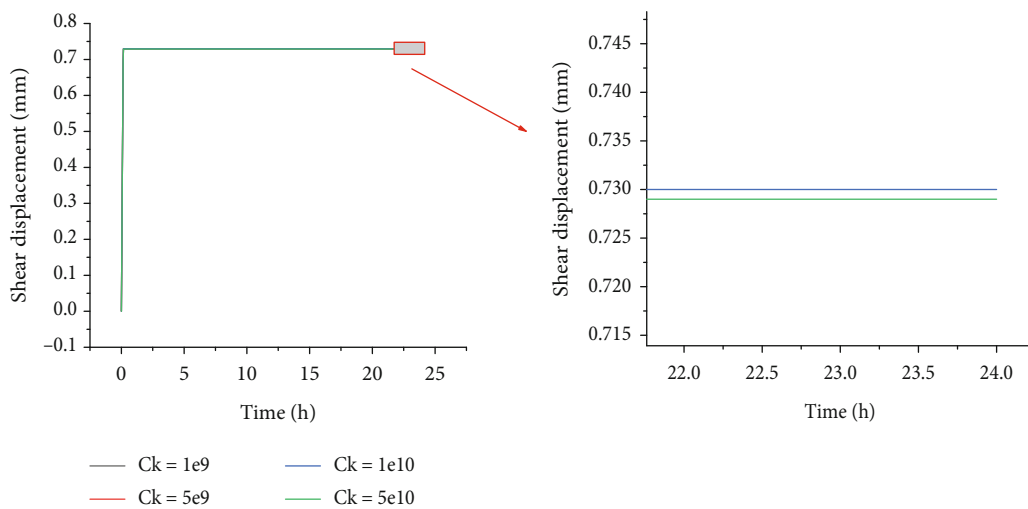


FIGURE 11: Shear displacement-time curves with bolts under different C_k conditions.

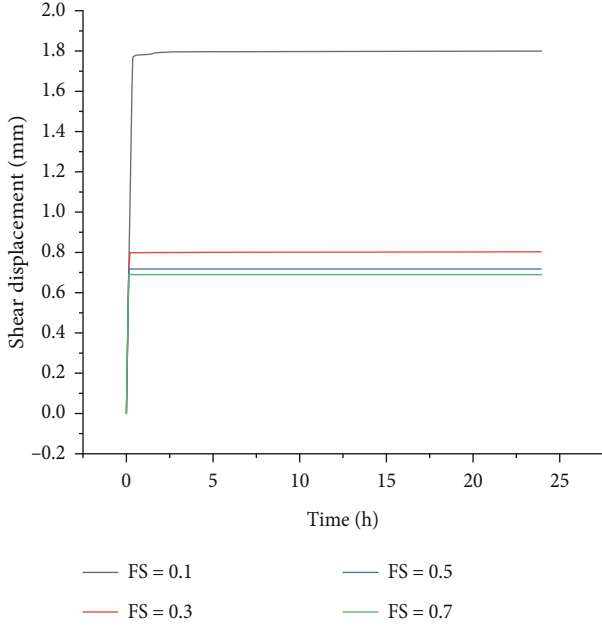


FIGURE 12: Shear displacement-time curves under different F_s conditions.

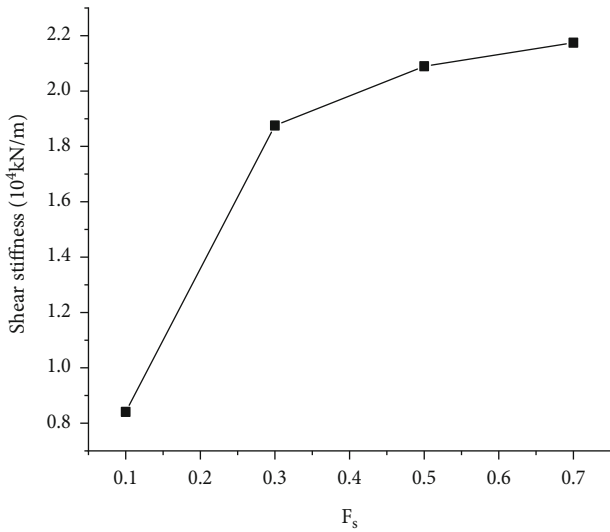


FIGURE 13: Relationship between F_s and shear stiffness.

Therefore, when the time range is not very large and E_k is not very small, the displacement affected by E_k is not particularly obvious. The relationship between shear displacement and time at different E_k was recorded, as shown in Figure 9. It can be seen from Figure 9 that E_k has little influence on instantaneous shear displacement, but has obvious influence on rheological shear displacement. The larger E_k is, the smaller the rheological shear displacement is, and there is a negative correlation between them. The rheological shear simulation results of bolted joints obtained by changing E_k show that adjusting E_k has no obvious effect on the numerical model displacement and crack of the joints. The results show that E_k affects the shear mechanical properties under

rheological conditions, but the effect is small when no damage occurs. Compared with the condition without bolt, the rock mass displacement with bolt is less affected by E_k .

3.4. Relationship between Joint Shear Displacement and Time under Different Kelvin Body Viscosity Coefficients. The Kelvin viscosity coefficient C_k affects the aging displacement of the contact between particles. The analysis of the microscopic parameters C_k of the contact between particles can effectively study the reflection of the parameters of Burger's model on the macroscopic shear mechanical properties of joints. Control variable method was adopted, set as $1E9$, $5E9$, $1E10$, and $5E10$, respectively, to analyze the sensitivity characteristics of Kelvin body viscosity coefficient C_k . Shear displacement-time curves under different C_k conditions are shown in Figure 10. It can be seen that C_k has little influence on instantaneous shear displacement, but significant influence on rheological shear displacement. The larger C_k is, the smaller the rheological shear displacement is, and there is a negative correlation between the two.

The rheological shear simulation results of unbolted joints obtained by changing C_k show that adjusting C_k has no significant effect on the joint numerical model displacement, crack. The results show that C_k affects the shear mechanical properties under rheological conditions, but the effect is small when no damage occurs. C_k is a factor affecting particle contact, but different from the displacement affected by E_m , the displacement affected by C_k is controlled by time. Therefore, when the time scale is not very large and C_k is not very small, the displacement affected by C_k is not particularly obvious. Shear displacement-time curves of bolted joints under different C_k conditions are shown in Figure 11. It can be seen that C_k has little influence on instantaneous shear displacement, but significant influence on rheological shear displacement. The larger C_k is, the smaller the rheological shear displacement is, and there is a negative correlation. The rheological shear simulation results of bolted joints obtained by changing C_k show that adjusting C_k has no significant effect on the joint numerical model displacement and crack. The results show that C_k affects the shear mechanical properties under rheological conditions, but the effect is small when no damage occurs. Compared with the condition without bolt, the rock mass displacement with bolt is less affected by C_k .

3.5. Influence of Joint Friction Coefficient on Joint Mechanical Behavior. In the rheological contact model, the friction coefficient affects the contact force between particles, and the analysis of the friction coefficient can effectively study the reflection of the rheological model parameters on the macroscopic shear mechanical properties of joints. The control variable method was adopted, set to 0.1, 0.3, 0.5, and 0.7, respectively, to analyze the sensitivity characteristics of friction coefficient F_s . Shear displacement-time curves under different F_s conditions are shown in Figure 12. As can be seen from the figure, the instantaneous shear displacement decreases with the increase of F_s , and F_s has a significant impact on the instantaneous shear displacement. The rheological shear displacement corresponding to

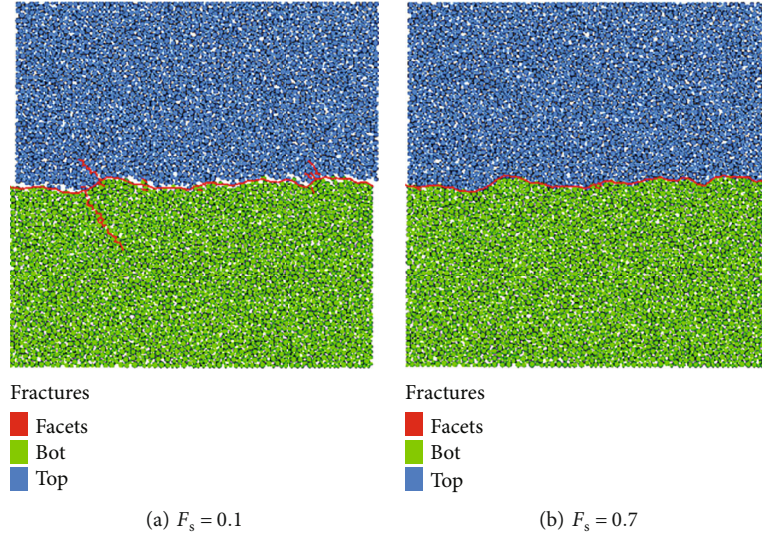


FIGURE 14: Number of sample cracks under different friction coefficients F_s .

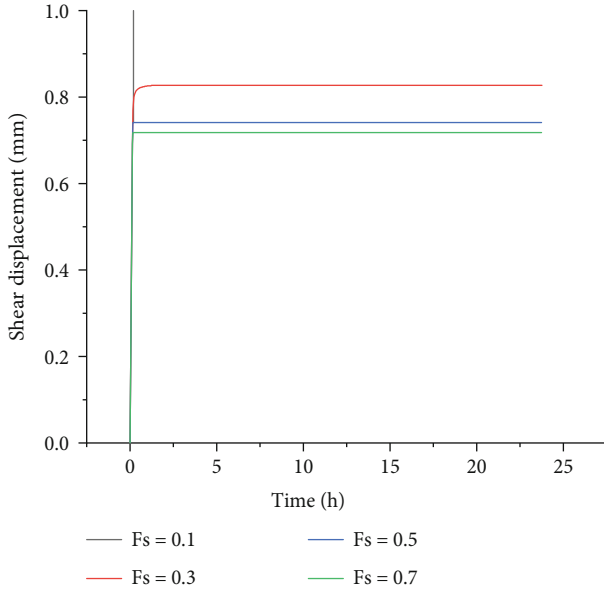


FIGURE 15: Shear displacement-time curves of different F_s with bolt.

different F_s is roughly the same, and F_s has no effect on the rheological shear displacement. By analyzing the elastic moduli corresponding to different F_s , the macroscopic shear stiffness corresponding to different F_s is obtained, and the relationship between F_s and shear stiffness is shown in Figure 13. It can be seen that there is a nonlinear relationship between F_s and the macroscopic shear stiffness, and the shear stiffness changes greatly, indicating that F_s has a significant impact on the macroscopic shear stiffness. The nonlinear expression is used to fit it, and the results are shown in Equation (3); R^2 is 0.99, indicating that the formula can well predict the macroscopic shear stiffness under different F_s conditions.

$$K_s = 2.77(1 - \exp(-7.3F_s)) - 0.59. \quad (3)$$

Respectively, change the interparticle friction coefficient of F_s , by calculation, the joint can be obtained corresponding crack number, displacement, as shown in Figure 14. It shows that, in the process of shearing, joint displacement and number of crack are significantly affected by F_s . The greater the shear displacement is smaller, the less crack. F_s has a negative relationship with shear displacement and crack number. In the rheological model, the shear strength is controlled by the normal stress and friction coefficient F_s . Therefore, the larger F_s is, the greater the static friction force to overcome under the condition of the same displacement caused by particle contact is, and it is less likely to produce sliding and cracks.

In the case of bolted joint, shear displacement-time curves under different F_s conditions are shown in Figure 15. As can be seen from the figure, the instantaneous shear displacement decreases with the increase of F_s , and F_s has a significant impact on the instantaneous shear displacement. The rheological shear displacement corresponding to different F_s is roughly the same, and F_s has no effect on the rheological shear displacement. By analyzing the elastic moduli corresponding to different F_s , the macroscopic shear stiffness corresponding to different F_s is obtained, and the relationship between F_s and shear stiffness is shown in Figure 16. It can be seen that there is a nonlinear relationship between F_s and the macroscopic shear stiffness, and the shear stiffness changes greatly, indicating that F_s has a significant impact on the macroscopic shear stiffness. The nonlinear expression is used to fit it, and the results are shown in Equation (4); R^2 is 0.99, indicating that the formula can well predict the macroscopic shear stiffness under different F_s conditions. Compared with Formula (3) without bolt, the shear stiffness with bolt is less affected by F_s , and the anchor can reduce the influence of joint parameter F_s on mechanical properties.

For bolted joints, F_s is changed separately, and it is found that the larger F_s is, the smaller the shear displacement is, the fewer the cracks are, and the less obvious the tension chain

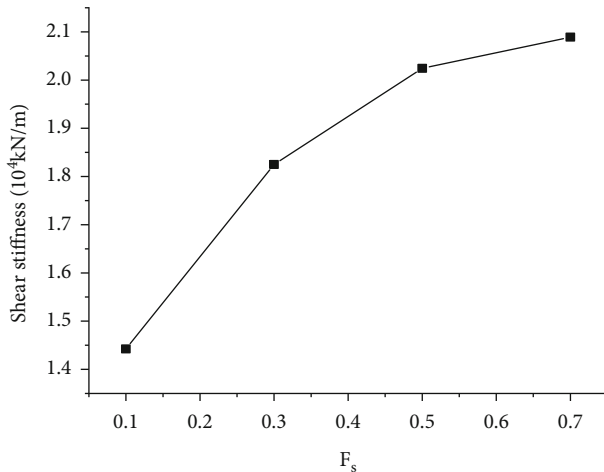


FIGURE 16: Relationship between F_s and shear stiffness.

concentration on the joints is. F_s has a negative relationship with shear displacement and crack number. Shear strength is controlled by normal stress and friction coefficient F_s and is proportional to F_s . Therefore, the larger F_s is, the more static friction force to be overcome under the condition of the same displacement caused by particle contact and the less prone to sliding and cracking of rock mass. However, the rock mass under the condition of anchor is less affected by F_s than that without bolt, and the anchor can reduce the influence brought by the change of rock mass mesoscopic parameters, which is conducive to enhancing the stability of rock mass.

$$K_s = 1.06[1 - \exp(-3.86F_s)] + 1.09. \quad (4)$$

4. Conclusions

- (1) For unbolted joint, E_m and F_s mainly affect the instantaneous shear displacement, but have little effect on the rheological shear displacement. However, C_m , E_k , and C_k have little effect on the instantaneous shear displacement, and the sensitivity is mainly reflected in the rheological shear displacement
- (2) For bolted joint, E_m and F_s mainly affect the instantaneous shear displacement, but have little effect on the rheological shear displacement. However, C_m , E_k , and C_k have little effect on the instantaneous shear displacement, and the sensitivity is mainly reflected in the rheological shear displacement. It should be noted that the instantaneous shear displacement, shear stiffness, and steady rheological displacement with bolt are less affected by parameters than the parameter sensitivity without bolt, indicating that the anchor can reduce the influence of joint parameters

Data Availability

The data used to support the findings of this study are available from the corresponding author upon request.

Conflicts of Interest

The authors declare no conflicts of interest.

References

- [1] X. Zhang, H. Lin, Y. Wang, R. Yong, Y. Zhao, and S. Du, "Damage evolution characteristics of saw-tooth joint under shear creep condition," *International Journal of Damage Mechanics*, vol. 30, no. 3, pp. 453–480, 2021.
- [2] S. Zare, S. Karimi-Nasab, and H. Jalalifar, "Analysis and determination of the behavioral mechanism of rock bridges using experimental and numerical modeling of non-persistent rock joints," *International Journal of Rock Mechanics and Mining Sciences*, vol. 141, p. 104714, 2021.
- [3] Y. Tang, H. Lin, Y. Wang, and Y. Zhao, "Rock slope stability analysis considering the effect of locked section," *Bulletin of Engineering Geology and the Environment*, vol. 80, no. 9, pp. 7241–7251, 2021.
- [4] H. Mansouri and R. Ajalloeian, "Mechanical behavior of salt rock under uniaxial compression and creep tests," *International Journal of Rock Mechanics and Mining Sciences*, vol. 110, pp. 19–27, 2018.
- [5] X. Fan, H. Yu, Z. Deng, Z. He, and Y. Zhao, "Cracking and deformation of cuboidal sandstone with a single nonpenetrating flaw under uniaxial compression," *Theoretical and Applied Fracture Mechanics*, vol. 119, article 103284, 2022.
- [6] Y. Zhao, Y. Wang, W. Wang, L. Tang, Q. Liu, and G. Cheng, "Modeling of rheological fracture behavior of rock cracks subjected to hydraulic pressure and far field stresses," *Theoretical and Applied Fracture Mechanics*, vol. 101, pp. 59–66, 2019.
- [7] M. Zambrano, A. D. Pitts, A. Salama, T. Volatili, M. Giorgioni, and E. Tondi, "Analysis of fracture roughness control on permeability using SfM and fluid flow simulations: implications for carbonate reservoir characterization," *Geofluids*, vol. 2019, Article ID 4132386, 19 pages, 2019.
- [8] E. Komurlu and A. Kesimal, "Experimental study on usability of friction rockbolts with plastic bodies," *International Journal of Geomechanics*, vol. 17, no. 9, p. 04017058, 2017.
- [9] H. Lin, W. Xiong, Z. Xiong, and F. Gong, "Three-dimensional effects in a flattened Brazilian disk test," *International Journal of Rock Mechanics and Mining Sciences*, vol. 74, pp. 94–100, 2019.
- [10] Z. Wen, E. Xing, S. Shi, and Y. Jiang, "Overlying strata structural modeling and support applicability analysis for large mining-height stopes," *Journal of Loss Prevention in the Process Industries*, vol. 57, no. 10-4, 2015.
- [11] D. Han, K. Li, and J. Meng, "Evolution of nonlinear elasticity and crack damage of rock joint under cyclic tension," *International Journal of Rock Mechanics and Mining Sciences*, vol. 128, article 104286, 2020.
- [12] D. Han, Y.-f. Leung, and J. Zhu, "Tensile strength and deformational behavior of stylolites and mineral healed joints subject to dynamic direct tension," *Rock Mechanics and Rock Engineering*, vol. 55, 2022.
- [13] K. Li, Y. Cheng, Z. Y. Yin, D. Y. Han, and J. J. Meng, "Size effects in a transversely isotropic rock under Brazilian tests: laboratory testing," *Rock Mechanics and Rock Engineering*, vol. 53, no. 6, pp. 2623–2642, 2020.
- [14] H. Yang, H. Lin, Y. Wang, R. Cao, J. Li, and Y. Zhao, "Investigation of the correlation between crack propagation process and the peak strength for the specimen containing a single

- pre-existing flaw made of rock-like material,” *Archives of Civil and Mechanical Engineering*, vol. 21, no. 2, p. 68, 2021.
- [15] Y. Chen, H. Lin, X. Ding, and S. Xie, “Scale effect of shear mechanical properties of non-penetrating horizontal rock-like joints,” *Environmental Earth Sciences*, vol. 80, no. 5, p. 1, 2021.
- [16] J. Meng, J. Huang, S. Sloan, and D. Sheng, “Discrete modelling jointed rock slopes using mathematical programming methods,” *Computers and Geotechnics*, vol. 96, pp. 189–202, 2018.
- [17] J. Jin, P. Cao, Y. Chen, C. Pu, D. Mao, and X. Fan, “Influence of single flaw on the failure process and energy mechanics of rock-like material,” *Computers and Geotechnics*, vol. 86, pp. 150–162, 2017.
- [18] C. Zhang, Y. Wang, and T. Jiang, “The propagation mechanism of an oblique straight crack in a rock sample and the effect of osmotic pressure under in-plane biaxial compression,” *Arabian Journal of Geosciences*, vol. 13, no. 15, p. 736, 2020.
- [19] X. Fan, Z. Yang, and K. Li, “Effects of the lining structure on mechanical and fracturing behaviors of four-arc shaped tunnels in a jointed rock mass under uniaxial compression,” *Theoretical and Applied Fracture Mechanics*, vol. 112, article 102887, 2021.
- [20] V. Sarfarazi, S. Abharian, and E. Z. Ghalam, “Physical test and PFC2D simulation of the failure mechanism of echelon joint under uniaxial compression,” *Computers and Concrete*, vol. 27, pp. 99–109, 2021.
- [21] A. S. Tawadrous, D. Degagné, M. Pierce, and I. D. Mas, “Prediction of uniaxial compression PFC3D model micro-properties using artificial neural networks,” *International Journal for Numerical and Analytical Methods in Geomechanics*, vol. 33, no. 18, pp. 1953–1962, 2009.
- [22] J. Shang, Z. Zhao, and S. Ma, “On the shear failure of incipient rock discontinuities under CNL and CNS boundary conditions: insights from DEM modelling,” *Engineering Geology*, vol. 234, pp. 153–166, 2018.
- [23] X. Zhang, H. Lin, Y. Wang, and Y. Zhao, “Creep damage model of rock mass under multi-level creep load based on spatio-temporal evolution of deformation modulus,” *Archives of Civil and Mechanical Engineering*, vol. 21, no. 2, p. 71, 2021.
- [24] M. Behnia, B. Nateghpour, J. Tavakoli, and B. M. Sharifi, “Comparison of experimental and empirical methods for estimating the shear strength of rock joints based on the statistical approach,” *Environmental Earth Sciences*, vol. 79, no. 14, p. 361, 2020.
- [25] R. Hao, P. Cao, Y. Chen, J. Jin, H. Wang, and X. Fan, “Mechanical and propagating behaviors of single-flawed rock samples with hydraulic pressure and uniaxial compression conditions,” *International Journal of Geomechanics*, vol. 18, no. 7, article 04018078, 2018.
- [26] N. Che, H. Wang, and M. Jiang, “DEM investigation of rock/bolt mechanical behaviour in pull-out tests,” *Particuology*, vol. 52, pp. 10–27, 2020.